

Influence of Nanoscopic Micellar Confinements and Rotational Dynamics of Anticancer Drug Doxorubicin

D.K. Rana*

Department of Chemistry, Saldaha College, Bankura-722173, West Bengal, India

(Received 21 May 2022, Accepted 23 July 2022)

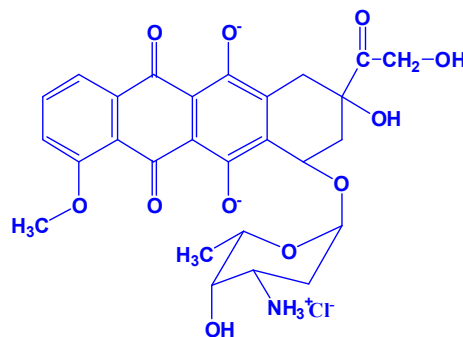
Modulation of photophysical properties and entrapping of fluorescence drug molecules in microheterogeneous systems are embracing potential applications in therapeutic pursuit. The present contribution describes the fascinating photo behaviour of an anticancer drug Doxorubicin (DOX) in micellar solutions of cationic cetyltrimethylammonium bromide (CTAB), anionic sodium dodecyl sulfate (SDS) and non-ionic p-tert-octylphenoxy polyoxyethanol (TX-100) surfactants by means of steady state, time-resolved emission and emission anisotropy procedures. Drug resides at the micelle-water interface in all these micellar systems as revealed by the fluorometric studies. Steady-state anisotropy and rotational relaxation time enhance in the micellar environment compared to it in pure aqueous solution revealing that the drug presents in a motionally constrained environment.

Keywords: Doxorubicin, Micelle, Lifetime, Anisotropy, Rotational relaxation

INTRODUCTION

Doxorubicin ((7S,9S)-7-[(2R,4S,5S,6S)-4-amino-5-hydroxy-6-methyloxan-2-yl]oxy-6,9,11-trihydroxy-9-(2-hydroxyacetyl)-4-methoxy-8,10-dihydro-7H-tetracene-5,12-dione) (Scheme 1) has attracted abundant attention in the field of medicinal research due to the treatment of different types of cancers, including liver carcinomas, breast, gastric, esophageal, osteosarcoma, Kaposi's sarcoma, Hodgkin's and non-Hodgkin's lymphomas, bile-duct carcinoma, pancreatic and endometrial carcinomas, and soft tissue sarcomas [1-4]. DOX is a component of the anthracycline group of antibiotics. It shows chemotherapeutic activity and avoids replication by causing conformational modifies in the DNA molecule through intercalating between adjacent DNA base pairs [5].

Currently, due to the capacity to develop *in vitro*, the response of several resistant cell lines to the transported drug,



Scheme 1. The chemical structure of the DOX is examined in the present study

DOX and its derivatives have extensively employed as anticancer drugs [6-8]. Owing to the inherently fluorescent nature of doxorubicin, it is suitable for probing and visualization with a variety of microscopic imaging techniques [9].

It is helpful to ascertain a relationship between the microenvironment and the photophysics of DOX, to illustrate how the drug is transported to its target. This will facilitate

*Corresponding author. E-mail: dipakranaju@gmail.com

one to observe the uptake of DOX by a specified carrier and its release from the carrier to a target site by monitoring the modification in absorption and fluorescence spectra. Unfortunately, photophysical properties of DOX have been reported by a few scattered studies [10-12]. Some studies have monitored the DOX fluorescence within cultured cells [13-17] and others have focused on the binding of DOX to DNA [18-22]. These works afford a partial perception of the photophysical properties of DOX within the micellar microenvironment.

Molecular confinement interpretations attractive properties in aqueous solution by means of its association and dynamics which are very unlike from that experienced in bulk water. Organized assemblies having nano dimensions acquire numerous distinctive features in comparison to a homogeneous mixture of solvents or a solitary solvent. The most important property of an organized assembly in spectroscopy is that the drug molecules which are usually sparingly soluble or insoluble in a pure bulk solvent, can stabilize and bind drug molecules in presence of surfactant [23]. Several studies reported that micelles exhibit different invincible advantages as potential drug delivery methods for weakly soluble pharmaceuticals [24,25]. Due to the hydrophobic nature of the core of the micelles, it is used as a cargo space for encapsulation of a diversity of drug molecules. Insightful interest has been drawn to the micellar systems due to micellar atmospheres have close similarity with biological systems such as enzymes, proteins, *etc.* [26,27]. Modification of photoprocesses has been made due to the encapsulation of the biologically potent molecules into the different biomimetic nano assemblies from bulk water since the polarity and viscosity in the microenvironment around the drug are different from those of the bulk aqueous phase [28]. Entrapping of drug molecules within micellar assemblies draws attention to exploring the prospective efficiency of its emission activities for the indulgence of its interaction with related biological targets.

With these viewpoints, we herein explore the photophysical properties of DOX in the micellar microenvironment created by anionic SDS, cationic CTAB, and non-ionic TX-100 using steady state and time-resolved fluorescence analysis. Our intention is to characterize different micellar bioassemblies entrapped DOX molecule and to interpret how the photophysical process changes

around the drug in micellar environment. Microviscosity around the DOX has been elucidated to find the rigidity of the DOX in different constrained environments. To appreciate the rotational behaviour of the DOX in confined media, we also intend to envisage its dynamics of it in these micellar environments. The present efforts also claim the potential applications of DOX as a fruitful extrinsic molecular reporter for microheterogeneous confinements.

MATERIALS AND METHODS

The anticancer drug Doxorubicin was procured from Fluka (Oakville, Canada) and it is employed without any further purification. CTAB and TX-100 were purchased from Aldrich; SDS was procured from BDH and was used as received. The concentration was of the order of 10^{-6} M of the drug used in water and micellar solution.

Shimadzu (model UV-1700) UV-Vis spectrophotometer and a Spex fluorolog-2 (model FL3-11) spectrofluorimeter with an external slit width of 2.5 mm were used to collect absorption and emission spectra. Determination of fluorescence lifetimes was made from time-resolved intensity decay by the technique of time-correlated single-photon counting employing a nanosecond diode laser at 403 nm (IBH, picoLED-07) as a source of light. The characteristic response time of the laser system at 403 nm was 70 ps. The information was routinely transferred to IBH DAS-6 decay analysis software which was stored in a multichannel analyzer. The emission decay curves were analyzed by single and biexponential iterative fitting programs for lifetime measurements supplied by IBH such as

$$F(t) = \sum_i \alpha_i \exp(-t/\tau_i) \quad (1)$$

where α_i stands for pre-exponential factor signifying fractional contribution to the time-resolved decay of the component with a lifetime τ_i . Mean (average) lifetimes $\langle \tau \rangle$ for bi-exponential decays of fluorescence was calculated from the decay times and pre-exponential factors using the subsequent Eq. (2)

$$\langle \tau \rangle = \frac{\alpha_1 \tau_1 + \alpha_2 \tau_2}{\alpha_1 + \alpha_2} \quad (2)$$

Horiba Jobin Yvon fluoromax-4 spectrofluorometer was used to carry out the steady-state fluorescence anisotropy measurements. Steady-state anisotropy (r) was calculated using the expression

$$r = (I_{VV} - GI_{VH}) / (I_{VV} + 2GI_{VH}) \quad (3)$$

where I_{VV} and I_{VH} are the intensities acquired from the excitation polarizer oriented vertically and the fluorescence polarizer oriented in vertical and horizontal directions, respectively. The factor G is characterized as $G = I_{HV}/I_{HH}$. All transients were taken by means of commercially obtainable (IBH) picosecond-resolved time-correlated single photon counting (TCSPC) setup (instrument response time ~ 80 ps) for anisotropy decay measurements. The picosecond excitation pulse from the diode laser was employed at 440 nm. Time-dependent fluorescence anisotropy $r(t)$ was calculated by the subsequent Eq. (4)

$$r(t) = [I_{VV}(t) - GI_{VH}(t)] / [I_{VV}(t) + 2GI_{VH}(t)] \quad (4)$$

where G corresponds to the grating factor of the fluorescence monochromator of the TCSPC method. All the experiments were carried out at ambient temperature (298 K).

RESULTS AND DISCUSSION

Steady State Measurements

DOX in aqueous solution exhibits two absorption bands, one strong band at 480 nm which arises because of charge transfer transition, and another weak band at 346 nm. On successive addition of the surfactants to the aqueous solution of DOX, the $\lambda_{\max}^{\text{abs}}$ value of charge transfer bands varies from

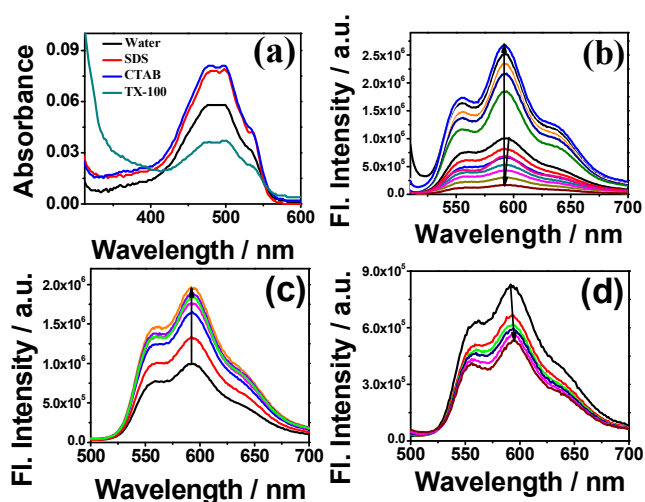


Fig. 1. (a) Absorption spectra of DOX in water, SDS, CTAB, and TX-100; (b) Emission spectra of DOX as a function of SDS concentrations, (c) Emission spectra of DOX as a function of CTAB concentrations, (d) Emission spectra of DOX as a function of TX-100 concentrations. In all cases, $\lambda_{\text{exc}} = 480$ nm.

479 to 485 nm (Fig. 1). These absorptions are sensitive to the polarity of the medium.

The fluorescence spectra of DOX in aqueous solution exhibit a structured band with a maximum at 593 nm. The fluorescence signature of DOX as a function of surfactant concentration has been represented in Fig. 1 and the corresponding spectral characteristics of DOX in different micellar environments are tabulated in Table 1.

With an increase in the concentration of anionic surfactants (SDS) in an aqueous solution of the DOX, the emission intensity shows a little initial drop followed by a huge enhancement together with a little hypsochromic shift.

Table 1. Spectral Characteristics, CMC Values, Binding Constant (K) Fluorescence Anisotropy (r), and Microviscosity ($\bar{\eta}$) of DOX in Different Micellar Environments

Environment	Emission maximum (nm)	CMC (mmol dm ⁻³)		$K \times 10^{-6}$ (mol ⁻¹ dm ⁻³)	r	$\bar{\eta}$ (cp)
		Exp	Lit ^{ref}			
SDS	592	8.60	8.20	7.82	0.15	1.70
CTAB	593	0.82	0.80	0.09	0.067	0.55
TX-100	594	0.29	0.27	2.86	0.18	2.37

An initial decrease in the emission intensity of the fluorophore is kind of common at the lower concentrations of assorted surfactants and is attributed to the formation of pre-micellar aggregates [28,29]. Addition of cationic surfactants (CTAB) in an aqueous solution of the DOX, the fluorescence intensity increases together with a minute hypsochromic shift. But in the case of non-ionic surfactant (TX-100), successive addition of surfactant in an aqueous solution of the DOX, the emission intensity decreases with small red shift. In anionic surfactant, enhancement of emission intensity is larger than the cationic micelles. A comparison of the observed emission maximum of DOX in the microheterogeneous environment to that in aqueous solution indicates the microenvironments in the region of the drug within the micellar phase are quite different from those in the pure aqueous solutions. This might be attributed to the microencapsulation of DOX into the micellar medium, which consequences in the change within the microenvironment experienced by this drug molecule. Changes of the microenvironment consist of the lower dielectric constant, polarity, high viscosity, and poor hydrogen bonding donor ability [29]. Because the drug DOX enters the micelle from bulk water the hydrogen bond gets stymied in the less polar hydrophobic environment and thereby the radiationless transition becomes less active and enhancement of ICT emission in ionic micelles ensues. But in the case of non-ionic micelles, hydrogen bond formation with the polar oxyethylene group and thereby the radiationless transition becomes active enough and diminishes of ICT emission in non-ionic micelles take place.

Variation of emission spectra of DOX in the presence of surfactant is little for low concentration of surfactant but this band gets affected significantly after a particular concentration. The critical micellar concentration (CMC) may be estimated from the alteration of relative emission intensity with the concentration of surfactants presented in Fig. 2 and also the CMC values summarised in Table 1. The calculated CMC values for SDS, CTAB, and TX-100 convincingly match to the values found in the literature [29] and therefore this result facilitates us using DOX as a fluorescent probe for micellar onset in aqueous environment.

The modification of emission intensity of DOX in the micellar medium is able to be reorganized in respect of binding of the drug with the micelle. But the strength of the

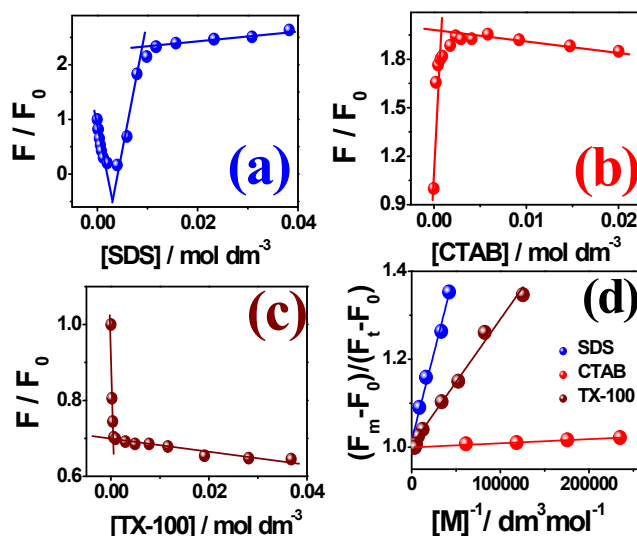


Fig. 2. Plot of relative fluorescence intensity versus concentration of surfactants (a) SDS; (b) CTAB; (c) TX-100. (d) Plot of $(F_m - F_0)/(F_t - F_0)$ of DOX in SDS, CTAB and TX-100 vs. $1/[M]$.

binding can be rationalized in terms of the binding constant between the drug and the micelle. From the emission intensity data following the method described by Almgren *et al.* [30] the binding constants between the drug and the micelles have been calculated.

$$\frac{F_m - F_0}{F_t - F_0} = 1 + \frac{1}{K[M]} \quad (5)$$

where F_t , F_0 , and F_m are the fluorescence intensities of DOX in presence of surfactant, in absence of surfactant, and under of fully micellization conditions, respectively. K stands for the binding constant between the drug and micelle. Using the surfactant concentration $[S]$ as $[M] = ([S] - \text{CMC})/n$ where n is the aggregation number, the micellar concentration $[M]$ has been calculated. The values of n for SDS, CTAB, and TX-100 have been taken as 62, 60 and 143, respectively from the literature [29]. The plot of $(F_m - F_0)/(F_t - F_0)$ against $1/[M]$ in relation to equation (Fig. 2) shows linear variation.

From the slopes of the individual plots, the binding constants (K) have been determined and the values (Table 1) follow the order of micelles $\text{SDS} > \text{TX-100} > \text{CTAB}$. The estimated binding constant values ($\pm 10\%$) fall into the range

of the values for some other systems reported [21]. Relatively stronger binding between the DOX and SDS micelle can be explained by the fact that DOX in neutral form has a partial positive charge, which interacts strongly with the negatively charged SDS micellar units.

Steady-State Fluorescence Anisotropy

Determination of fluorescence anisotropy performs a very crucial part in affecting the shape, size, or segmental flexibility of a molecule. As it directly reveals any motional restriction imposed on the drug by the environment, steady-state fluorescence anisotropy of DOX has been studied in various micellar microenvironments. Figure 3 illustrates the variation of fluorescence anisotropy (r) of DOX as a function of micellar concentration and also the data were collected in Table 1.

An imposed motional restriction on the fluorophore within the micellar systems has been revealed from the rise of fluorescence anisotropy of the drug molecule with an increasing micellar concentration. The drug molecule bound to the micelle tumbles much slowly compared to the free drug in water, and hence anisotropy increases when the surfactant concentration is increased. This observation indicates some specific interactions centered surrounding the drug and also the hetero atoms present within the surfactant, resulting to the trapping of the drug in some motionally constrained site of the micelles or some additional restriction imposed on the motion of the overall molecule. The extent of anisotropy change monitored in the case of SDS and TX-100 is remarkably higher than the extent of the changes observed in CTAB media. This reveals that the drug is comparatively more confined within the former microenvironments.

We have calculated the microviscosity ($\bar{\eta}$) using the following Eq. (6) [31] since the fluorescence anisotropy of a fluorescent drug molecule is closely connected with the viscosity of the microenvironment around it.

$$\bar{\eta} = \frac{2.4r}{0.362-r} \quad (6)$$

where (r) corresponds to the fluorescence anisotropy of DOX in the micellar microenvironment. The calculated microviscosity of micelle-bound DOX are illustrated in Table 1.

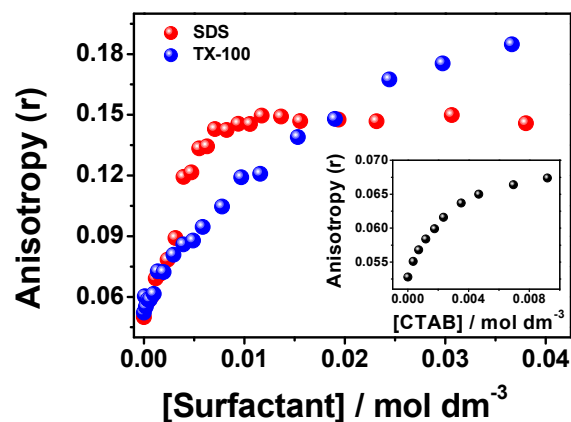


Fig. 3. Variation of fluorescence anisotropy (r) of DOX as a function of SDS and TX-100 concentrations. Inset represents the same for CTAB. $\lambda_{\text{exc}} = 480$ nm.

Time-Resolved Fluorescence Decay

Fluorescence lifetime provides an admirable indicator to examine the position of the drug in a multi-component environment. Differential degrees of solvent relaxation in the region of the drug in separate regions of a confined environment generate differences in the fluorescence lifetime of the drug. So using time-resolved emission study photophysical response of the DOX in micellar media compared to aqueous environment has been confirmed.

DOX shows single exponential decay in aqueous and bi-exponential decays in micellar environments. Figure 4 represents the excited singlet state decay signatures of DOX in aqueous and micellar environments. In the micellar environments, the lifetime values of the drug are significantly longer than those in pure aqueous solution and the lifetime values are represented in Table 2.

Extraction of meaningful rate constants in such heterogeneous systems is difficult. As observed in the case of binding with the micelles in the previous section, the average lifetime enhances with raising the concentration of surfactant. Lifetime increases with increasing the concentration of SDS micelles which was also observed in the case of binding with the micelles in the previous section. An increase in the fluorescence lifetime in SDS compared to in CTAB and TX-100 micelles may be due to the formation of ionic complex for which binding constant of the probe with the micelles differ.

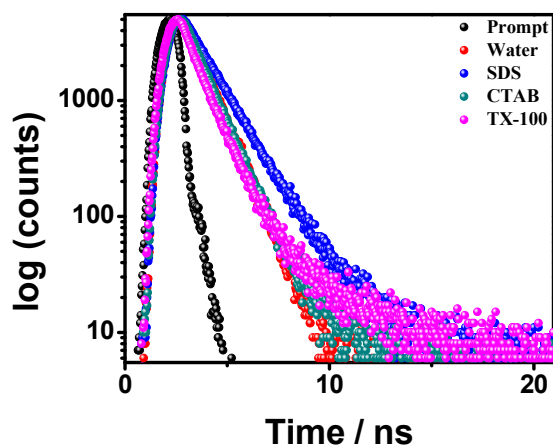


Fig. 4. (a) Typical emission decay curves of DOX associated with lamp profile in the water, SDS, CTAB, and TX-100 micellar environments, respectively; $\lambda_{ex} = 480$ nm.

Table 2. Fluorescence Lifetime of DOX in Aqueous and Micellar Microenvironments along with Normalized Pre-Exponential Factors

Environment	α_1	τ_1 (ns)	α_2	τ_2 (ns)	$\langle\tau_{av}\rangle$ (ns)	χ^2
Water	1.00	1.02	-	-	1.02	1.23
SDS	0.945	1.27	0.055	2.7	1.35	1.15
CTAB	0.972	0.95	0.028	2.3	0.988	1.14
TX-100	0.977	0.84	0.023	3.27	0.895	1.14

Time-Resolved Fluorescence Anisotropy Decay

Significant insights about the rotational dynamism and rotational relaxation of the drug in organized systems have been acquired from the time-resolved decay of the fluorescence anisotropy. To rationalize how the rotational relaxation dynamics of this drug are affected when ongoing from bulk aqueous phase to the micellar solution, fluorescence anisotropy decays of DOX in water and as well as in micellar environment were measured.

Figure 5 represents the fluorescence anisotropy decays of DOX in water and various micellar microenvironments and respective decay parameters are collected in Table 3.

The anisotropy decays are found to display single

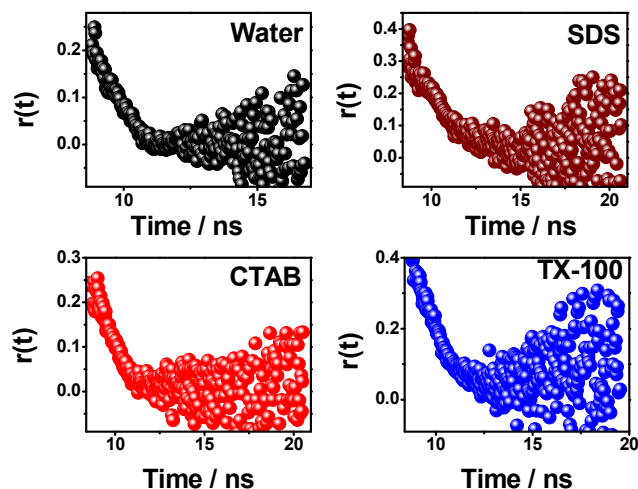


Fig. 5. Time-resolved fluorescence anisotropy decay profiles for DOX in water, SDS, CTAB, and TX-100. The excitation laser source is set at 440 nm.

Table 3. Rotational Relaxation time of DOX in Aqueous and Micellar Media and along with Hydrodynamic Radii (r_h), Reorientation Times (τ_M) of the Micelle

Environment	β	$\langle\tau_r\rangle$ (ns)	χ^2	r_h^a (Å)	τ_M^a (ns)
Water	1.00	1.13	1.11	-	-
SDS	1.00	2.49	1.13	20.7	8.3
CTAB	1.00	1.29	1.27	25.7	15.4
TX-100	1.00	1.28	1.14	43.0	72.0

^aValues are taken from reference [29].

exponential decay patterns in all the investigated environments. Functional form of anisotropy decay $r(t)$ (single exponential) is given by the subsequent Eq. (7)

$$r(t) = r_0 \exp(-t/\tau_r) \quad (7)$$

where τ_r is the reorientation time and r_0 is the limiting anisotropy which depends on the inherent depolarisation of the fluorophore. DOX shows a considerably longer rotational relaxation time in micelles than that in pure water as reflected in Fig. 5 and Table 3. This is because of the fact that DOX endures motionally restricted environments imposed by the micelles. Table 3 reveals that the rotational relaxation times

(τ_r) in all cases are greater than the fluorescence lifetimes of DOX in corresponding environments, indicating the completion of the relaxation processes within the lifetime of the photoexcited state of the drug molecule.

Anisotropy relaxation of a drug in a micellar media may convey the following possibilities for instance (a) drug molecules rotate within the micelles, (b) the encapsulated drug does not rotate but the micelles bounding the drug rotate, and (c) together rotation of micelles and drug are possible. In the case of first and second choice, single exponential decay patterns should result whereas the third alternative leads to biexponential anisotropy decay. Single exponential anisotropy decays of DOX fluorescence in aqueous and aqueous micellar solution, thus leaving out the third preference. Using the Stokes-Einstein-Debye (SED) Eq. (8) [27] the rotational relaxation times of the micelles (τ_M) can be calculated.

$$\tau_M = \frac{4\pi\eta r_h^3}{3kT} \quad (8)$$

Where η implies the viscosity of water (in poise), r_h is the hydrodynamic radius of the micelle, and k and T are the Boltzmann constant, and absolute temperature, respectively and the consequent data are summarised in Table 3. Table 3 reveals that the rotational relaxation times of the micelles are appreciably larger than the consequent depolarization times of emission in the micellar media. This evidence additionally supports that the relaxation of the emission anisotropy results from the rotation of the drug molecule only and not of the micelles. The τ_r values follow the order SDS < CTAB < TX-100.

CONCLUSIONS

The photophysical and rotational dynamical behaviour of anticancer drug DOX in ionic and non-ionic micelles has been explored using steady-state, time-resolved fluorescence, and fluorescence anisotropy study. Modulation of the photophysics of DOX produced by the micelles is significantly larger for emission spectral trend compared to ground state absorption properties. This significant modulation of the microenvironment of the drug has been effectively utilized in determining the drug-micelle binding.

Anionic micelle SDS exhibits much greater binding efficiency relative to TX-100 and CTAB micelles. Time-resolved decay of DOX also reveals that the excited singlet state is affected more in SDS micellar environment than TX-100 and CTAB micellar environments. Time-resolved anisotropy ascertains the diversity in rotational relaxation of DOX entrapped in various micellar assemblies. This insight will also facilitate opening up new opportunities for the transport mechanism in the organized microenvironment for targeted delivery of the anticancer drug DOX.

ACKNOWLEDGEMENTS

I am grateful to Prof. S. C. Bhattacharya, Jadavpur University for his kind permission and assistance during the experimental work. I am also thankful to Dr. Sayaree Dhar, Jadavpur University for her cooperation and support throughout the experimental work.

REFERENCES

- [1] Minotti, G.; Menna, P.; Salvatorelli, E.; Cairo, G.; Gianni, L., Anthracyclines: molecular advances and pharmacologic developments in antitumor activity and cardiotoxicity. *Pharmacol. Rev.* **2004**, *56*, 185-229, DOI: 10.1124/pr.56.2.6.
- [2] Ewer, M.; Ewer, S., Cardiotoxicity of anticancer treatments: what the cardiologist needs to know. *Nat. Rev. Cardiol.* **2010**, *7*, 564-575, DOI: 10.1038/nrcardio.2010.121.
- [3] Candido, N. M.; de Melo, M. T.; Franchi, L. P.; Primo, F. L.; Tedesco, A. C.; Rahal, P.; Calmon, M. F., Combining Photodynamic Therapy and Chemotherapy: Improving Breast Cancer Treatment with Nanotechnology. *J. Biomed. Nanotech.* **2018**, *14*(5), 994-1008, DOI: 10.1166/jbn.2018.2558.
- [4] Tap, W. D.; Wagner, A. J.; Schöffski, P.; Martin-Broto J.; Krarup-Hansen, A.; Ganjoo, K. N.; Yen, C. C.; Razak, A. R. A.; Spira, A.; Kawai, A.; Cesne A. L.; Tine, B. A. V.; Naito, Y.; Park, S. H.; Fedenko, A.; Pápai Z.; Soldatenkova V.; Shahir A.; Mo, G.; Wright, J.; Jones, R. L., Effect of Doxorubicin Plus Olaratumab vs. Doxorubicin Plus Placebo on Survival in Patients With Advanced Soft Tissue Sarcomas The Announce

- Randomized Clinical Trial. *Jama Original Investigation* **2020**, *323*(13), 1266-1276, DOI: 10.1001/jama.2020.1707.
- [5] Box, V. G. S., The intercalation of DNA double helices with doxorubicin and nagalomycin. *Journal of Molecular Graphics and Modelling* **2007**, *26*(1), 14-19, DOI: 10.1016/j.jmgm.2006.09.005.
- [6] Nguyen, H. X.; Bozorg, B. D.; Kim, Y.; Wieber, A.; Birk, G.; Lubda, D.; Banga, A. K., Poly (vinyl alcohol) microneedles: Fabrication, characterization, and application for transdermal drug delivery of doxorubicin. *European Journal of Pharmaceutics and Biopharmaceutics* **2018**, *129*, 88-103, DOI: 10.1016/j.ejpb.2018.05.017.
- [7] Calcagno, A. M.; Fostel, J. M.; To, K. K.; Salcido, C. D.; Martin, S. E.; Chewning, K. J.; Wu, C. P.; Varticovski, L.; Bates, S. E.; Caplen, N. J.; Ambudkar, S. V., Single-step doxorubicin-selected cancer cells over express the ABCG2 drug transporter through epigenetic changes. *Br. J. Cancer* **2008**, *98*(9), 1515-1524, DOI: 10.1038/sj.bjc.6604334.
- [8] O'Shaughnessy, J., Extending Survival with Chemotherapy in Metastatic Breast Cancer. *Oncologist* **2005**, *10*, 20-29, DOI: 10.1634/theoncologist.10-90003-20.
- [9] Lebold, T.; Jung, C.; Michaelis, J.; Bra"uchle, C., Nanostructured Silica Materials As Drug-Delivery Systems for Doxorubicin: Single Molecule and Cellular Studies. *Nano Lett.* **2009**, *9*(8), 2877-2883, DOI: 10.1021/nl9011112.
- [10] Rana, D. K.; Dhar, S.; Sarkar, A.; Bhattacharya, S. C., Dual Intramolecular Hydrogen Bond as a Switch for Inducing Ground and Excited State Intramolecular Double Proton Transfer in Doxorubicin: An Excitation Wavelength Dependence Study. *J. Phys. Chem. A* **2011**, *115*, 9169-9179, DOI: 10.1021/jp204165j.
- [11] Liu, X.; Zhao, J.; Zheng, Y., Insight into the excited-state double proton transfer mechanisms of doxorubicin in acetonitrile solvent. *RSC Adv.* **2017**, *7*, 51318-51323, DOI: 10.1039/c7ra08945g.
- [12] Behera, S. K.; Mohanty, M. E.; Mohapatra, M., A Fluorescence Study of the Interaction of Anticancer Drug Molecule Doxorubicin Hydrochloride in Pluronic P123 and F127 Micelles. *Journal of Fluorescence* **2021**, *31*, 17-27, DOI: 10.1007/s10895-020-02630-y.
- [13] Lovitt, C. J.; Shelper T. B.; Avery V. M., Doxorubicin resistance in breast cancer cells is mediated by extracellular matrix proteins. *BMC Cancer* **2018**, *18*, 41-51, DOI: 10.1186/s12885-017-3953-6.
- [14] Peng, Z.; Nie, K.; Song, Y.; Liu, H.; Zhou, Y.; Yuan, Y.; Chen, D.; Peng, X.; Yan, W.; Song, J.; Qu, J., Monitoring the Cellular Delivery of Doxorubicin-Cu Complexes in Cells by Fluorescence Lifetime Imaging Microscopy. *J. Phys. Chem. A* **2020**, *124*(21), 4235-4240, DOI: 10.1021/acs.jpca.0c00182.
- [15] Wei, H.; Chen, J.; Wang, S.; Fu, F.; Zhu, X.; Wu, C.; Liu, Z.; Zhong, G.; Lin, J., A Nanodrug Consisting Of Doxorubicin And Exosome Derived From Mesenchymal Stem Cells For Osteosarcoma Treatment *In Vitro*. *Int. J. Nanomedicine* **2019**, *14*, 8603-8610, DOI: 10.2147/IJN.S218988.
- [16] Kalimuthu, S.; Zhu, L.; Oh, J. M.; Gangadaran, P.; Lee, H. W.; Baek, S. H.; Rajendran, R. L.; Gopal, A.; Jeong, S. Y.; Lee, S. W.; Lee, J.; Ahn, B. C., Migration of mesenchymal stem cells to tumor xenograft models and *in vitro* drug delivery by doxorubicin. *Int. J. Med. Sci.* **2018**, *15*(10), 1051-1061, DOI: 10.7150/ijms.25760.
- [17] Barros, A. S.; Costa, E. C.; Nunes, S.; Diogo, D. M.; Correia, I. J., Comparative study of the therapeutic effect of Doxorubicin and Resveratrol combination on 2D and 3D (spheroids) cell culture models. *Int. J. Pharm.* **2018**, *551*, 76-83, DOI: 10.1016/j.ijpharm.2018.09.016.
- [18] Zhang, X.; Poniewierski, A.; Sozański, K.; Zhou, Y.; Elliott, A. B.; Holyst, R., Fluorescence correlation spectroscopy for multiple-site equilibrium binding: a case of doxorubicin-DNA interaction. *Phys. Chem. Chem. Phys.* **2019**, *21*, 1572-1577, DOI: 10.1039/c8cp06752j.
- [19] Kalar, Z. M.; Yavari, A.; Jouyban, A., Increasing DNA binding affinity of doxorubicin by loading on Fe₃O₄ nanoparticles: A multi-spectroscopic study. *Spectrochimica Acta Part A: Molecular and Biomolecular Spectroscopy* **2020**, *229*, 117985-117993, DOI: 10.1016/j.saa.2019.117985.
- [20] Arnaiz, C. P.; Busto, N.; Leal, J. M.; García B., New Insights into the Mechanism of the DNA/Doxorubicin Interaction. *J. Phys. Chem. B* **2014**, *118*(5), 1288-1295,

DOI: 10.1021/jp411429g.

- [21] Jawad, B.; Poudel, L.; Podgornik, R.; Steinmetz, N. F.; Ching, W. Y., Molecular mechanism and binding free energy of doxorubicin intercalation in DNA. *Phys. Chem. Chem. Phys.* **2019**, *7*, 1-17, DOI: 10.1039/c8cp06776g.
- [22] Ijäs, H.; Shen, B.; Jungemann, A. H.; Keller, A.; Kostianen, M. A.; Liedl, T.; Ihalainen, J. A.; Linko, V., Unraveling the interaction between doxorubicin and DNA origami nanostructures for customizable chemotherapeutic drug release. *Nucleic Acids Research* **2021**, *49*(6), 3048-3062, DOI: 10.1093/nar/gkab097.
- [23] Banerjee, P.; Pramanik, S.; Sarkar, A.; Bhattacharya, S. C., Modulated Photophysics of 3-Pyrazolyl-2-pyrazoline Derivative Entrapped in Micellar Assembly. *J. Phys. Chem. B* **2008**, *112*, 7211-7219, DOI: 10.1021/jp800200v.
- [24] Torchilin, V. P., Structure and design of polymeric surfactant-based drug delivery systems. *J. Controlled Release* **2001**, *73*, 137-172, DOI: 10.1016/s0168-3659(01)00299-1.
- [25] Gao, Z.; Lukyanov, A. N.; Singhal, A.; Torchilin, V. P., Diacyllipid-Polymer Micelles as Nanocarriers for Poorly Soluble Anticancer Drugs. *Nano Lett.* **2002**, *2*, 979-982, DOI: 10.1021/nl025604a.
- [26] Sahoo, D.; Chakravorti, S., Influence of surfactants on the excited state photophysics of 4-nitro-1-hydroxy-2-naphthoic acid. *Photochem. Photobiol. Sci.* **2010**, *9*(8), 1094-1100, DOI: 10.1039/c0pp00104j.
- [27] Lakowicz, J. R., *Principles of Fluorescence Spectroscopy*. third ed., Springer, New York, **2006**.
- [28] Das, P.; Chakrabarty, A.; Mallick, A.; Chattopadhyay, N., Photophysics of a Cationic Biological Photosensitizer in Anionic Micellar Environments: Combined Effect of Polarity and Rigidity. *J. Phys. Chem. B* **2007**, *111*(38), 11169-11176, DOI: 10.1021/jp073984o.
- [29] Dhar, S.; Rana, D. K.; Bhattacharya, S. C., Influence of nanoscopic micellar confinements on spectroscopic probing and rotational dynamics of an antioxidative naphthalimide derivative. *Colloids and Surfaces A: Physicochem. Eng. Aspects* **2012**, *402*, 117-126, DOI: 10.1016/j.colsurfa.2012.03.035.
- [30] Almgren, M.; Grieser, F.; Thomas, J. K., Dynamic and static aspects of solubilization of neutral arenes in ionic micellar solutions. *J. Am. Chem. Soc.* **1979**, *101*(2), 279-291, DOI: 10.1021/ja00496a001.
- [31] Wang, X.; Wang, J.; Wang, Y.; Yan, H., Effect of the Nature of the Spacer on the Aggregation Properties of Gemini Surfactants in an Aqueous Solution. *Langmuir* **2004**, *20*(1), 53-56, DOI: 10.1021/la0351008.